Freeman Gebler, O., Hicks, B., Harrison, A., & Barker, M. (2017). Investigating the diagnostic capabilities of monitored system parameters to support improvements in conveyor operation and maintenance. Paper presented at First World Congress on Condition Monitoring, London, United Kingdom.

Peer reviewed version

License (if available):
Unspecified

University of Bristol - Explore Bristol Research
General rights

Investigating the diagnostic capabilities of monitored system parameters to support improvements in conveyor operation and maintenance

Owen Freeman Gebler[1,2], Ben Hicks, Andrew Harrison
University of Bristol[1]
Bristol, BS8 1TR, England
07783719702
o.freemangebler@bristol.ac.uk

Matt Barker
Stirling Dynamics[2]
Bristol, BS8 4HG, England

Abstract

This paper investigates the potential value of a range of system parameters in supporting improvements in operation and maintenance practices of conveyor systems. To achieve this a conveyor emulation rig (CER) is developed to emulate the dynamics of a typical industrial conveyor system and allow the controlled application of a range of loading conditions and fault scenarios typical of general processing industries.

Initially, the design and specification of the rig is discussed, after which data is presented and analysed in the context of characterising the operational envelope of the system as well as supporting fault detection, isolation and typing tasks. For the purpose of this paper, the operational conditions employed to characterise the system include variations of radial, axial and braking loads, and types of seeded fault include component damage and environmental changes.

Results suggest that individual parameters present sensitivity to only a specific subset of scenarios and, as such, a greater fidelity of inference can potentially be achieved when the data from a range of parameters is considered in conjunction as opposed to each in isolation.

1. Introduction

Conveyor systems are ubiquitous assets, utilised throughout industry to provide the fundamental function of product transfer. Implementations range from the vast, kilometre length fixed systems in the mining industry, to product transfer systems in processing and packing plants, and portable systems used on domestic construction sites to clear excavated material.

While conveyor systems may not directly add value to a product their function within the overall process is critical for operation, and thus for value to flow. Typically a conveyor system will represent a single point of failure, where any inoperability will cause the en-

tire process to be halted. The cost of unplanned process downtime varies significantly between industries and applications, with determining an accurate quantification of the cost a challenge in itself, however it has been suggested that lost production within an open-pit mine can be as high as ~$300k/hr[1]. Consequently, availability demands on systems are stringent; operators need to be able to have confidence that systems are going to be operational on demand, thus avoiding potential for unplanned process downtime.

Due to the perceived utility of conveyor systems they are often operated in a flexible manner, with individual systems repurposed throughout a plant in response to process changes. In addition, it is not uncommon for a plant's production demands to increase over time, driven by high-level strategic factors[2]. As a result of this, systems are commonly exposed to a diverse operational envelope, where they are subjected to loadings, environmental conditions (e.g. temperature, humidity, airborne particulate) and conveyed products outside those considered in their design, which can result in the catastrophic and apparently random failure. This is compounded by the fact that operation and maintenance of conveyors may be conducted by untrained personnel who lack knowledge of the design envelope of a conveyor, and how to operate and maintain the system within this, thus further increasing the potential of 'abuse' loading and ultimately failure.

As a direct result of the significant variance in operational characteristics experienced by a conveyor, the failure modes observed in response can also be wide ranging and implementation specific. The failure of a system describes any occurrence which renders the system unable to satisfy its primary function. Within the context of a conveyor system a failure can thus be defined as any occurrence that impacts upon the ability of the system to satisfy its primary requirement of transferring product from one location to another.

As an example consider a completely severed belt; this occurrence will render a system unable to convey product and thus can be defined as a failure. However, in addition to such failures undesirable conditions can arise within a conveyor, which, while not necessarily rendering the system unable to satisfy its primary function, impact upon operations.

Such conditions are termed faults, describing any condition that occurs, which impacts upon the manner in which a system operates, but does not render the system immediately inoperable. For example, an idler can become seized during operation, leading to the development of a flat spot. This occurrence on its own will not necessarily prevent the conveyor from satisfying its primary requirement, however the sharp edges of the flat may ultimately cause damage to the belt eventually leading to complete system failure.

In contrast to the binary nature of failures, defining the point at which a fault within a system is considered to be present can be subjective and imprecise. This has significant impact upon the maintenance of the system, presenting a challenge to operators in determining the point at which to address a fault - too soon and an avoidable period of downtime will be incurred, too late and the fault may induce a failure with a potentially far greater period of associated downtime before primary function can be restored.

Failures and faults within conveyor systems can be classified at 4 primary levels:

- System – a failure or fault affecting the operation of an entire process

- Asset – a failure or fault affecting a specific conveyor's operation

- Component – a failure or fault affecting a specific element of a conveyor e.g. motor

- Feature – a failure or fault affecting a specific subcomponent within a conveyor component e.g. bearing inner race, motor rotor etc.

In most industries the corrective action in response to the occurrence of a failure or fault will be a component level replacement, regardless of whether a feature-level root cause can be determined. This is because the relatively low cost of components compared to the cost of downtime means that it is often more economical to replace immediately rather than repair or risk running components to failure. However, this is contingent on replacement components being available and a relatively low frequency of replacements. In some industries this practice is now being reviewed due to the significant cumulative cost of replacements. Consequentially, the low-value high-volume asset industries are now also seeking to improve their maintenance regimes and are looking at the potential of technologies such as reliability-centred maintenance (RCM) and prognostics and health management (PHM)[3],[4],[5],[6],[7].

For these operators the challenges of applying PHM is no less trivial than for high-value assets. This is because the form of the failure and fault conditions experienced by a conveyor system are influenced by the environment within which it's operated, including both its physical operational environment (e.g. temperature, humidity, product conveying etc.) as well as the manner in which it's operated (e.g. maintenance, utilisation etc.) which may be different to the operational envelope for which it was designed. It is thus necessary to understand the operational demand, as well as the type of failure, and assess these with respect to the designed capability. Further, and in contrast to operators of high-value low-volume assets, operators of low-value high-volume assets typically face considerably tighter financial constraints, meaning that any technology-based solutions must in themselves be low cost to implement and operate.

1.1. Conveyor Operation and Maintenance

In order to sustain high levels of availability of plant and equipment informed maintenance procedures are essential. The maintenance of an asset, within the broadest engineering context, can be considered to constitute any action taken to preserve the function of the asset, as required by its stakeholders[8]. Broadly, approaches to maintenance of assets can be divided into three major categories, ordered in increasing complexity of implementation: reactive (RM), planned preventative (PPM), and predictive (PM)[9].

Historically, approaches to the maintenance of conveyor systems have been dominated by RM and PPM-based schemes, due to their simplistic principles of implementation. Such schemes rely heavily upon human inspection ('walking the belt') to determine the operational health of assets[10],[11],[12], and, as such operators have little reliable, objective information about the usage of a conveyor upon which to base operational and maintenance decisions. The manner in which a conveyor system has been operated can be considered

to have a direct impact upon the wear and thus life of components, therefore the potential value of asset health information to operator is significant.

To address this deficiency operators are increasingly seeking to implement aspects of PM-based philosophies, where aspirations are that such a shift could allow for more objectivity within the tasks of condition/health assessment. In doing so, a range of benefits can potentially be realised, as reported widely within literature (see[13],[14],[15]). To support this shift operators will require an understanding of how conveyor systems are being used in an objective, quantifiable manner.

In order to support these industries and, in particular, operators of low-value high-volume assets we aim to explore the potential inferencing capability of range of typical sensors and the observability of system parameters they enable. To achieve this, the design and development of an experimental test rig, created for the purpose of emulating the dynamics of a typical small-scale industrial conveyor system is presented.

The paper begins with an analysis of how a typical conveyor system could be expected to fail to operate, leading to formulation of requirements for the functionality of the test rig. Then, an overview of the design and development process for the rig is provided and a testing regime to enable characterisation and the repeatable replication of a range of observed failure modes is presented.

Finally, data acquired during the completion of the testing regime is presented and the ability of each system parameter to support four levels of diagnostics is considered:

- Characterising the operational envelope of a system – how can the usage of a system be described and monitored using sensor data, when operating in a healthy state throughout its feasible loading conditions.

- Detecting the presence of system faults – using this characterisation of 'healthy' operation can the transition to an abnormal or 'unhealthy' state be identified using the information provided by sensors.

- Isolating the location of system faults – when the presence of an unhealthy operational state has been identified, can sensor data support the determination of the element within the system which is responsible for inducing the change in operational state.

- Determine the type of system faults – can the form of any faults that occur within the system be determined using information from sensors, enabling the identification of the root cause mechanism.

2.   The Conveyor Emulation Rig

To enable the detailed exploration of these tasks a test rig was developed. The conveyor emulation rig (CER) is designed to emulate the dynamics of a typical industrial conveyor system, and allow for the controlled introduction of modes of loading, reflective of those typically subjected to during operation. This research is not concerned with the condition assessment of belting material therefore a belt is omitted, however its presence can be replicated via applied loading.
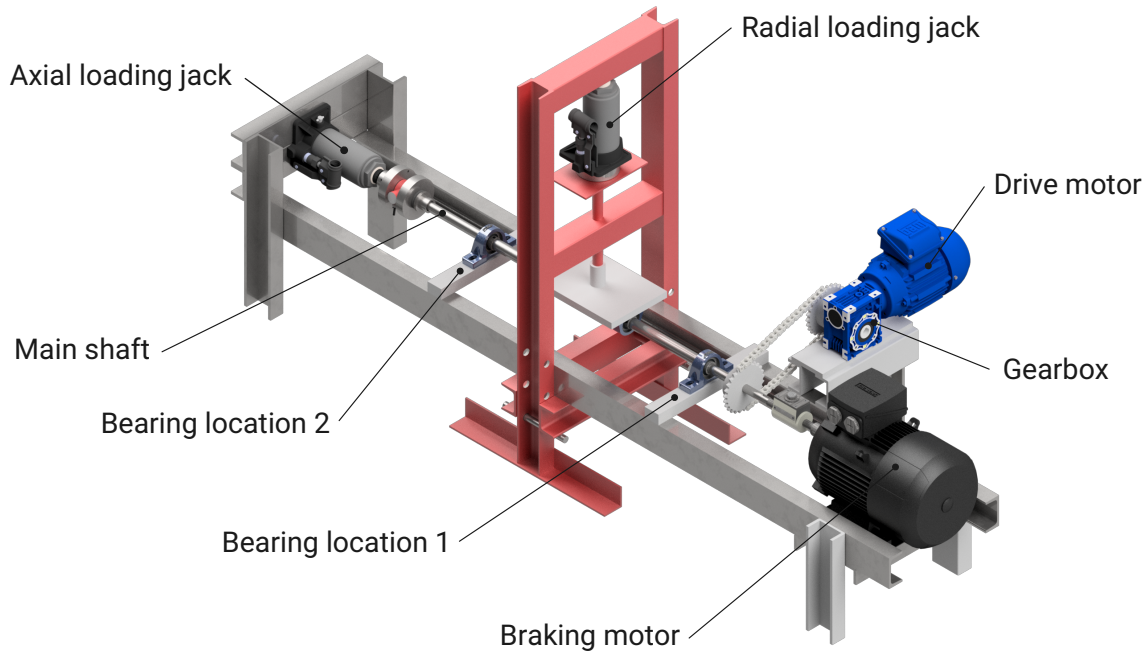

Figure 1: Render of CER with major elements labelled

2.1.   Requirements

To inform the design of the conveyor test rig requirements were derived from the form of failures and faults, as well as the loading envelope typically observed on an industrial conveyor system. To identify the possible failure and fault scenarios of a small-medium sized conveyor system, failure mode and effect analysis (FMEA) was conducted, based upon physics of failure and extant literature such as ISO 17359:2011[16].

From this initial exhaustive analysis a reduced set of failures and faults were selected (table 1), representing the most frequently encountered issues within industry, as determined through engagements with a conveyor manufacturer, as well as an operator within the waste management industry[11].

Table 1: Reduced set of failure modes of conveyor system

Asset		Function	Functional Failure (Loss of Function)		Failure Mode			Failure Effect		Relative time cost (1-5)
					Level 1	Level 2	Level 3	*What happens when it fails?*	*What action is required in reponse?*	
Drive motor	A	To provide mechanical power to the conveyor drive end shaft under a loaded motor condition at the required speed and torque, when a voltage is applied	1	Unable to provide the required output torque and speed magnitude	i	Overheating motor due to fan performance	Fan performance reduced	Fan outlet blocked	Motor housing internal temperature likely to rise potentaily inducing one of the failure modes above (I,ii,iii)	Clearing of blockage from outlet by operator	1
								Blade damaged		Replacement of fan and potetially motor dependent upon damage incurred	3-4
							Fan not operational	Fan blocked		Clearing of blockage from fan blade by operator	2
								All blades damaged		Replacement of fan and potetially motor dependent upon damage incurred	3-4
Gearbox	B	To transfer the required torque and speed from the motor	1	Reduced torque transfer efficiency compared to	i	Gear tooth damage	Abrasive action by debris		Conveyor can continue to operate but likely increase in parameters such as temp, vib,	Once levels are considered unacceptable a replacement will be required	3-4
							Corrosion present	Water ingress			
Driveshaft bearing	C	To support shaft loading whilst allowing free rotation of the driveshaft	1	Rotation reduced for a given input torque	i	Damaged race	Overheating causing annealing		Conveyor will continue to operate but at a lower speed likely (assuming no motor speed control) and thus throughput will be reduced. Additionally the drive components (gearbox, motor) are likely to incur increased load and thus increased wear	Replacement of the damaged bearing likely to be required	3-4
							Excessive loading				
							Excessive vibration	Misalignment in bearing/shaft			
								Debris ingress			
							Installation issue				
					ii	Lack of lubricant	Damaged seals			Depending on the magnitude of dmaaged incurred either a full replacement of the bearing or a	1-4
							Lack of maintenance				
							Supply line issue				
					iii	Debris ingress	Damaged seals			Cleaning of the bearing may improve condition however replacement likely to be required	1-4
					iv	Corrosion present	Water ingress			Replacement of the damaged bearing likely to be required	3-4
							Contaminent ingress				
							Age				
				2	No rotation possible	i	Bearing collapsed	Seal damage	Excessive loading	If a bearing is totally siezed either; the driveshaft and thus the conveyor belt will be halted or if the shaft detaches from the siezed bearing	Replacement of the damaged bearing likely to be required	3-4
							Age				
							Impact damage				
					ii	Bearing seized	Lack of lubricant			Replacement of the damaged bearing likely to be required	3-4
							Foreign body e.g. magnetic tape				
	D	To constrain the shaft axially thus transferring any axial loading	1	Shaft axial movement unconstrained	i	Bearing fastening failure	Installation issue		Belt ension will reduced, potentially causing it to come loose	Retightening of relevant fixtures	1--2
							Excessive vibration				
					ii	Bearing collapsed	Significant thrust load present	Uneven belt tension		Replacement of the damaged bearing likely to be required	3-4
							Lack of lubricant				

2.2. Specification

In its simplest form a conveyor system is composed of a driven (head) and passive (tail) pulley connected by a flexible belt, supported along the belt length by a number of passive rollers (idlers) (fig. 2). An induction motor is used to move the belt, via a reduction gearbox, to provide an appropriate level of torque and speed. Traditionally drive motors are driven at a fixed speed by a constant frequency supply, via a direct-on-line (DoL) starter however variable-speed inverter-driven systems are finding increasing implementation throughout general processing applications.
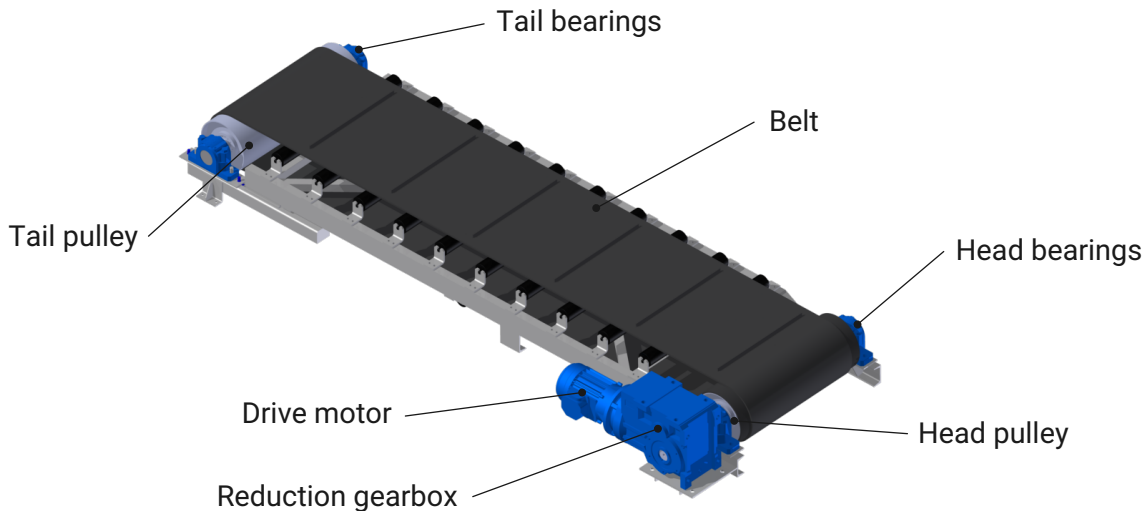

Figure 2: Major components comprising typical industrial conveyor system

The rig is specified to reflect a popular portable conveyor system configuration, as supplied by a range of UK manufacturers such as Coveya, Hoverdale and Robson. With this in mind, a specification describing the top-level physical and performance characteristics of the test rig was developed (table 2).

Table 2: Specification of Conveyor Emulation Rig

Belt Width	600mm	Motor Power	370W
Conveyor Length	3000mm	Motor Speed	1370rpm @ 50Hz
Conveyor Speed	~200rpm	Gearbox Ratio	7.5:1
Throughput	100ton/hr	Pulley Diameter	40-50mm

2.3. Component Specification

Where possible low cost, commercial-off-the-shelf (COTS) components were selected to ensure the rig reflected the make-up of an actual industrial system, as closely as possible.

To drive the test rig a Marelli 0.37kW, 3 phase, 240Vac powered induction motor of 'squirrel cage' construction form was selected, reflective of the form of drive motor commonly employed for industrial conveyor applications. The motor is an enclosed machine, with an IP55 protection rating, and is actively cooled using a permanently attached, on-shaft fan. The motor is powered by a Vacon 10 0.55kW variable-frequency drive, controlled

remotely by a PC via an RS485 connection. The inverter is operated in open loop V/f (Volts-per-Hertz) mode (i.e. no closed-loop speed control), to reflect the typical configuration of an industrial conveyor system. A VFD is selected over DoL connection due to its ability to modulate conveyor speed, enabling a range of belt speeds to be characterised.

Coupled to the motor is a TEC worm-drive gearbox, with a speed reduction ratio of 7.5:1 and 85% power efficiency, thus providing an output of approximately 183RPM and 16.4Nm of torque at 50Hz input. In contrast to a typical industrial conveyor system the unit is entirely sealed, with no external breather required for cooling purposes. To transfer the drive power from the gearbox to the drive shaft a sprocket and chain system is used. The sprocket set has a ratio of 1:3, thus it increases the speed output from the gearbox by a factor of 3. Mechanical wear within a bearing can be considered a function of applied load and number of rotations, therefore by increasing the output of the gearbox wear can be accelerated.

To support the test rig drive shaft a pair of single row, angular contact ball bearings are employed, housed within a 'plummer block' style unit. Typically a conveyor of the specification described in Table ASAS would have a pulley shaft diameter of around 40-50mm, however, to accelerate the effect of externally loading the bearings a reduced shaft, and thus bearing diameter of 20mm was selected. The bearings selected are manufactured by SKF and have a stated static load rating of 6.5kN. They are prelubricated, and provided with non-removable press-fit seals as well as a shield cover on either side. Within the CER the bearing in closest proximity to the drive motor is referred to as being in location 1, with the bearing farthest from the drive motor at location 2.

Table 3: CER major components

Component	Manufacturer	Manu. ID
Drive motor	Marelli	MAA71MB4 B14
Gearbox	TEC	FCNDK40-7.5:1-71B14
Shaft bearings	SKF	SY20 TF (housing unit), YAR 204-2F (bearing)

2.4. Loading Mechanisms

To enable the complete operational envelope of a conveyor system to be replicated on the test rig a series of loading mechanisms were designed. Analysis of the range of scenarios described in section 2.1 indicated that all could be replicated using a combination of axial, radial and torsional loading of the test rig drive shaft (table 4).

To facilitate the controlled application of radial load to the drive shaft the test rig employs a manually-operated hydraulic jack. When actuated, the radial jack applies a linear force to main shaft, distributed between the two support bearings, via a yoke.

Similarly, axial load can be applied to the drive shaft using a second hydraulic jack, transmitted via a needle roller thrust bearing, to minimise torsional friction. Each jack is capable of applying a maximum load of 30kN. However, due to the load-bearing ability of the drive shaft applied radial load is limited to 3kN, to minimise the risk of shaft fracture.

Finally, torsional load can be applied to oppose the drive motor via a second 4.8kW induc-

Table 4: Summary of loads required to replicate operational scenarios

Scenario	Impact	Replication
Varying quantity of product on belt	Increased load observed by motor and gearbox	Torsional loading of drive shaft
Overload trip and subsequent loaded restart of system	Starting torque requirement increased	Sudden stop of drive. Restart with torsional load present
Uneven tension in belt	Thrust load applied to drive shaft	Axial loading of shaft
Increased belt tension	Increase in static radial load on shaft	Increase radial load on drive shaft
Belt failure	Reduction in static radial load on shaft	Sudden reduction in radial load on shaft
Corrosion of bearings	Increased rolling resistance within bearing	Seed corroded bearing
Damaged bearing seal	Increased rolling resistance	Seed seal damage
		Inject debris into bearing
Overloaded bearing	Increased rolling resistance	Radially load bearing
		Seed overloaded bearing
Drivetrain obstructed by product	Cooling of drivetrain inhibited	Thermally inhibit drivetrain
Gearbox breather blocked	Reduction in cooling power of gearbox	Manually block breather
Gearbox component damage	Poor running of gearbox	Seed debris into gearbox during operation

tion motor, utilising the principle of direct current (DC) injection braking. By injecting DC into the stator coils of the braking motor a stationary magnetic field is generated, which acts to oppose the torque of the drive motor. The strength of the torsional load generated is controlled by modulating the amplitude of the DC injected, up to a maximum of 9A. As such, by employing a programmable power supply various braking load profiles can be applied (e.g. saw tooth) enabling the effect of different operational scenarios to be simulated. It should be noted that the braking power generated by the motor is a function of the applied current and the speed of the rotor; greater torque is produced as the speed is reduced. A sprocket set is used to transfer the output of the gearbox unit to the drive shaft. Whilst not reflective of a typical industrial system this setup allows for increased flexibility in operating the rig; by enabling access to both ends of the shaft both axial and braking loads can be applied simultaneously.

2.5. Instrumentation

Due to the exploratory nature of the research objectives it was desirable to continuously monitor a wide range of system parameters as potential proxies for health. Initially, a review of extant health monitoring literature was conducted to enable the identification of possible system parameters that could be monitored. The output of this review was then used, in conjunction with key reference materials[17],[18], to analyse the probable effect of each scenario on each system parameters (table 5).

Table 5: Response of system parameters to failure modes

Item	Failure mode	Root cause	Δ throughput	Δ belt speed	↑ system vibration	↑ system noise	vision (belt)	Δ roller speed	↑ motor current draw	↑ motor temp	Δ motor vibration	↑ motor torque	Δ motor speed	Δ motor leakage current	↑ gearbox oil temp	Δ gearbox oil analysis	Δ gearbox oil level	Δ gearbox vibration	↑ bearing temp	Δ bearing speed	Δ bearing vibration	bearing SPM	Δ bearing AE
Conveyor System	Reduced throughput	Increased friction due to seized roller	•	•	•	•		•	•	•		•											
Conveyor System	Reduced throughput	Increased friction due to collapsed bearing	•	•				•	•	•		•							•		•		
Conveyor System	Reduced throughput	Conveyor blocked	•	•	•		•	•	•	•		•											
Gearbox	Reduced transfer	Gear tooth damage due to debris			•	•			•		•					•		•			•		
Gearbox	Reduced transfer	Gear tooth damage due to corrosion								•						•		•			•		
Gearbox	No transfer	Gears seized due to overheating	•	•				•	•	•					•								
Bearing	Reduced rotation	Damaged race due to overheating			•	•		•	•				•		•				•	•	•	•	•
Bearing	Reduced rotation	Damaged race due to overloading	•					•	•			•	•		•				•	•	•	•	•
Bearing	Reduced rotation	Damaged race due to excessive vibration			•	•		•			•								•	•	•	•	•
Bearing	No rotation	Collapsed due to seal damage	•	•	•	•	•	•											•	•	•		•
Bearing	No rotation	Collapsed due to impact	•	•	•	•	•	•											•	•	•	•	•
Bearing	No rotation	Seized due to lack of lube	•	•	•	•	•	•											•	•	•		
Bearing	No rotation	Seized due to foreign object	•	•	•	•	•	•											•	•	•		

From this matrix a subset of parameters to monitor during operation of the CER was selected, based upon the expected richness of the information provided by each, as well as factors such as cost and implementability.

Table 6: Summary of CER instrumentation

	Monitored parameter	Sensor	Signal conditioning	Acquisition unit	Acquisition rate	Continuous / Periodic
Drive motor	Line voltages (VAB and VCA)	LEM LV25-P	Custom LP filter and amplifier unit	NI USB6211	10kHz /phase	C
	Phase currents (IA and IB)	LEM LA25-NP	Custom LP filter and amplifier unit	NI USB6211	10kHz /phase	C
	Casing temperature	PT100	Industrial Interface E100		2Hz	C
	Vibration	Dytran 3255A2	NI 9234		50kHz	P
Gearbox	Output shaft speed	Honeywell 103SR13A-1	NA	NI USB6211	Counter input	C
	Casing temperature	PT100	Industrial Interface E100		2Hz	C
	Audible noise	Bruel & Kjaer type 4117	NI 9234		50kHz	P
	Acoustic Emission	Mistras WD	Mistras 2/4/6C voltage amplifier	NI PCI9251	1MHz	P
Bearing 1	Casing temperature	PT100	Industrial Interface E100		2Hz	C
	Vibration	Dytran 3255A2	NI 9234		50kHz	P
	Audible noise	Bruel & Kjaer type 4117	NI 9234		50kHz	P
Bearing 2	Casing temperature	PT100	Industrial Interface E100		2Hz	C
	Vibration	Dytran 3255A2	NI 9234		50kHz	P
	Audible noise	Bruel & Kjaer type 4117	NI 9234		50kHz	P
Radial jack	Applied load	Tedea Huntleigh TH220	Soemer LAC65.1 amplifier	NI USB6211	1Hz	C
Axial jack	Applied load	Novatech F210	Vishay Nobel AST 3IS	NI USB6211	1Hz	C
Braking motor	Output power	Manson HCS-3302-USB	NA		2Hz	C
	Applied torsional load	HBM T5	Vishay Nobel AST3IS	NI USB6211	1Hz	C
Environment	Ambient temperature	PT100	Industrial Interface E-100		2Hz	C

All data acquisition devices are interfaced with a single control PC running a custom HMI within the National Instruments LabVIEW environment, enabling both operation of the test rig as well as handling all data acquisition tasks. All data acquired from operation of the test rig is stored both locally on the control PC as well as in the cloud, with the LabVIEW TDMS file format employed. Each test scenario run is assigned a unique ID and data is stored within a top-level folder, beneath which data is split into data sections. Individual test scenario folders can subsequently be imported into the Mathworks® MATLAB® package for analysis.

The rotational velocity of the gearbox output shaft is monitored using a non-contact Hall-effect sensor in conjunction with a custom magnet wheel. The rotational speed of the shaft is calculated from the time between sinking pulses, generated each time a magnet passes the sensor, and the know distance between magnets. The output of the speed sensor was calibrated prior to testing using a non-contact optical speed measurement device with a stated ±0.05% accuracy. Both outputs were found to be within 0.2RPM typically.
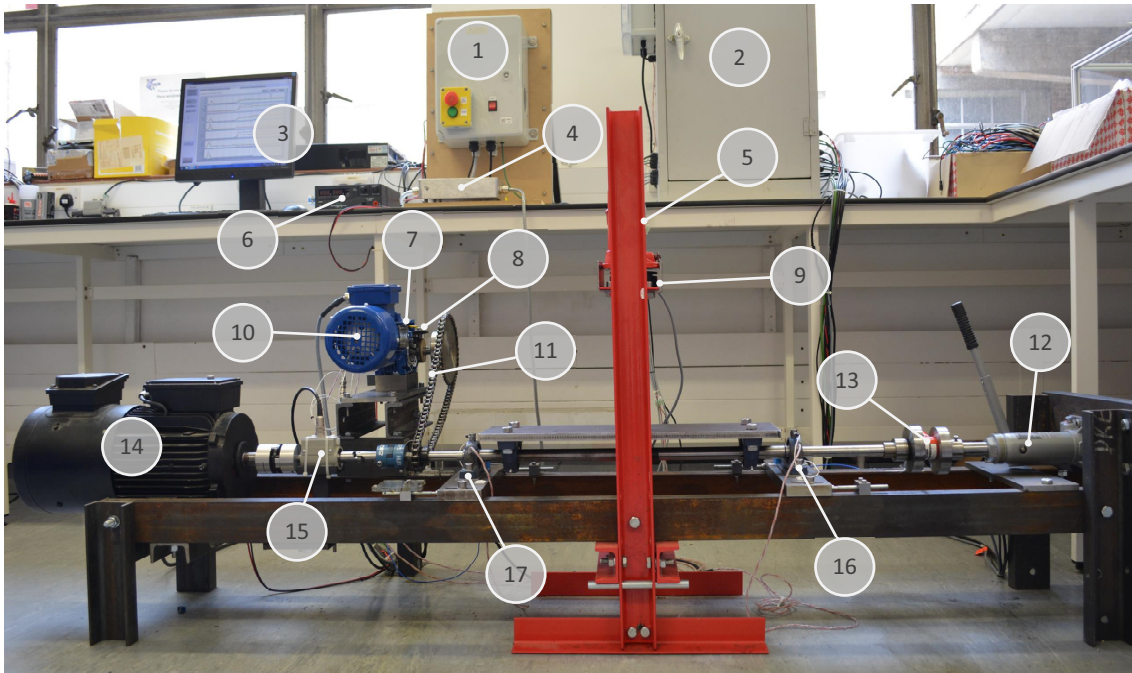
Figure 3: Overview of CER: 1 - VFD box; 2 - DAQ cabinet; 3 - Control PC and HMI; 4 - Power monitoring; 5 - Radial jack; 6 - DC injection power supply; 7 - Gearbox; 8 - Speed sensor; 9 - Radial loadcell; 10 - Drive motor; 11 - Drive chain; 12 - Axial jack; 13 - Axial loadcell; 14 - Braking motor; 15 - Torque transducer; 16 - Bearing 2; 17 - Bearing 1

The magnitude of linear (radial and axial) loads applied to the rig is measured using two compression-type load cells, with maximum measurement capacities of 25kN and 100kN respectively. The output of each cell was amplified using a dedicated amplifier and ultimately input into a National Instruments USB-6211 data acquisition device to enable real-time monitoring of applied loads. The output of each load cell amplifier was calibrated using an Instron 8872 testing machine, with a class 0.5% calibration rating, to enable accurate conversion from amplifier output voltage to absolute load.

Torsional load applied by the braking motor is measured using an in-line torque transducer, capable of measuring loads up to 20Nm, interfaced with a dedicated amplifier. The output of the torque transducer was calibrated using a rig at the University of Bristol, where a digital torque transducer was used to verify the accuracy of the CER transducer.

To enable the power waveforms output from the VFD to be monitored a custom acquisition unit was designed and constructed, allowing for the waveforms of 2 motor line voltages and 2 motor phase currents to be observed. By selecting the appropriate line voltages and phase currents to monitor (v_{ab}, v_{ca}, i_a, i_b) it can be shown that the instantaneous input power of a 3-phase induction motor can be determined from only 2 line voltages and 2 phase currents[19].

Power measurement is based around 4 closed-loop, Hall-effect COTS devices manufactured by LEM, with a measurable range and nominal accuracy of 250Vac RMS and 0.5%, and 5A RMS and 0.9% of full range, respectively. The output of each device is passed

through an active filtering stage, where a 2nd order low-pass filter with cutoff frequency of around 300Hz is applied to each channel. This serves to remove any high-frequency harmonics present within the waveforms as a result of the VFD switching action. The output of each channel was calibrated using a sinusoidal supply and a high precision Fluke 45 digital multimeter (DMM) and accuracy within 1% of full scale was observed for each.

The temperature of the primary rig components under test (drive motor, gearbox, bearing A and B), as well as the ambient temperature, are monitored using sealed PT100 probes, selected due to their excellent linearity and precision[20]. Each component probe has a measurement range of -200°C, and is bonded directly to the surface of its associated component using a metalised epoxy adhesive, to ensure good physical and thermal bonding is present (fig. 4). All probes are connected to a single signal conditioning unit, which outputs a converted, IEEE 754 floating point value per channel, pertaining to the measured absolute temperature.
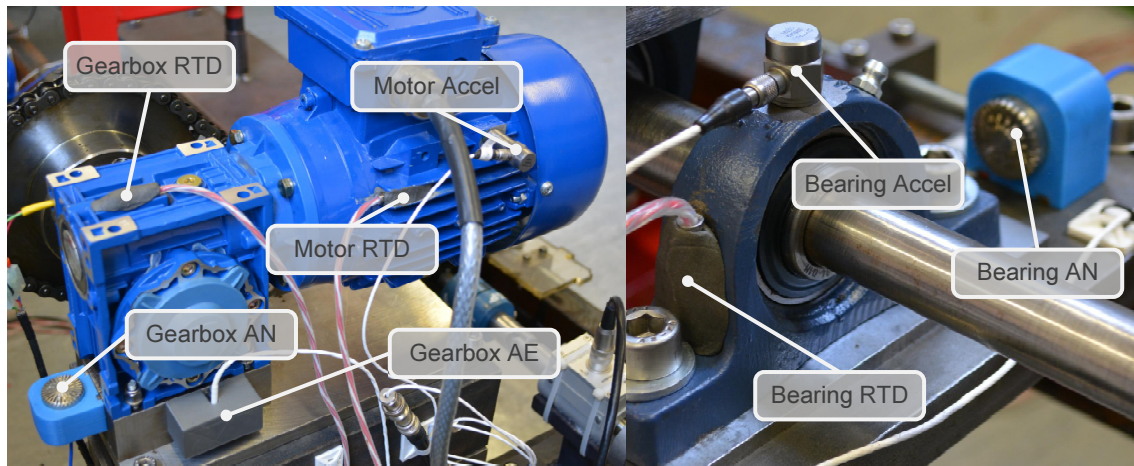

Figure 4: Locations of vibration, audible noise and acoustic emission sensors within CER

Single axis vibration of each of the drive motor and bearings A and B is monitored using a Dytran 3255A2 accelerometer. Each sensor is mounted directly to its monitored component using a threaded steel insert to ensure excellent mechanical fastening, and thus signal transmission. Additionally, silicon grease is used to reduce any attenuation[21]. For bearing measurements sensors are located top centre of each housing, measuring vibration in the Y axis, as suggested in[22]. For motor vibrations, suitable locations for threaded inserts are minimal; to overcome this a bespoke stainless steel adapter is employed, to enable an existing, unused threaded hole on the motor body to be used.

Each accelerometer is connected to a National Instruments NI 9234 data acquisition module, which employs built-in antialiasing filters, and configured to sample each channel at 50kHz. Similarly, each of the 3 audible noise sensors are connected to a second NI9234 module, again employing antialiasing filters and configured to a 50kHz sample rate. Audible noise sensors are housed within custom 3D printed mounts, coupled to their monitored components magnetically. As with the vibration monitoring, the drive motor presents no obvious location for mounting an audible noise sensor, and, along with the gearbox, is not magnetic, hence a sensor is located on the steel gearbox mount.

Finally, an acoustic emission sensor, manufactured by Physical Acoustics, is used to monitor gearbox meshing activities. The sensor is of wideband differential specification, providing a good response between frequencies of 100-900kHz. The sensor's output is amplified using an inline voltage preamplifier, set to a gain of 20dB, and ultimately interfaced with a National Instruments PCI6251 data acquisition card, where it is sampled at a rate of 1.25MHz. The sensor is mounted exactly as the gearbox audible noise sensor, directly to the gearbox mount, and again silicone grease is employed to improve signal transmission.

To reduce the volume of data acquired during operation of the rig, whilst avoiding the attenuation of potentially valuable, high frequency content contained within parameters, certain sensors were sampled periodically. For vibration, audible noise and acoustic emission parameters samples were taken in a 1 second period, every 30 seconds.

Vibration, audible noise and acoustic emission parameters were sampled periodically (30s), in order to reduce data volumes whilst avoiding the attenuation of high frequency content within these parameters. Additionally, this phase of research shall focus solely upon time-domain analysis of signals.
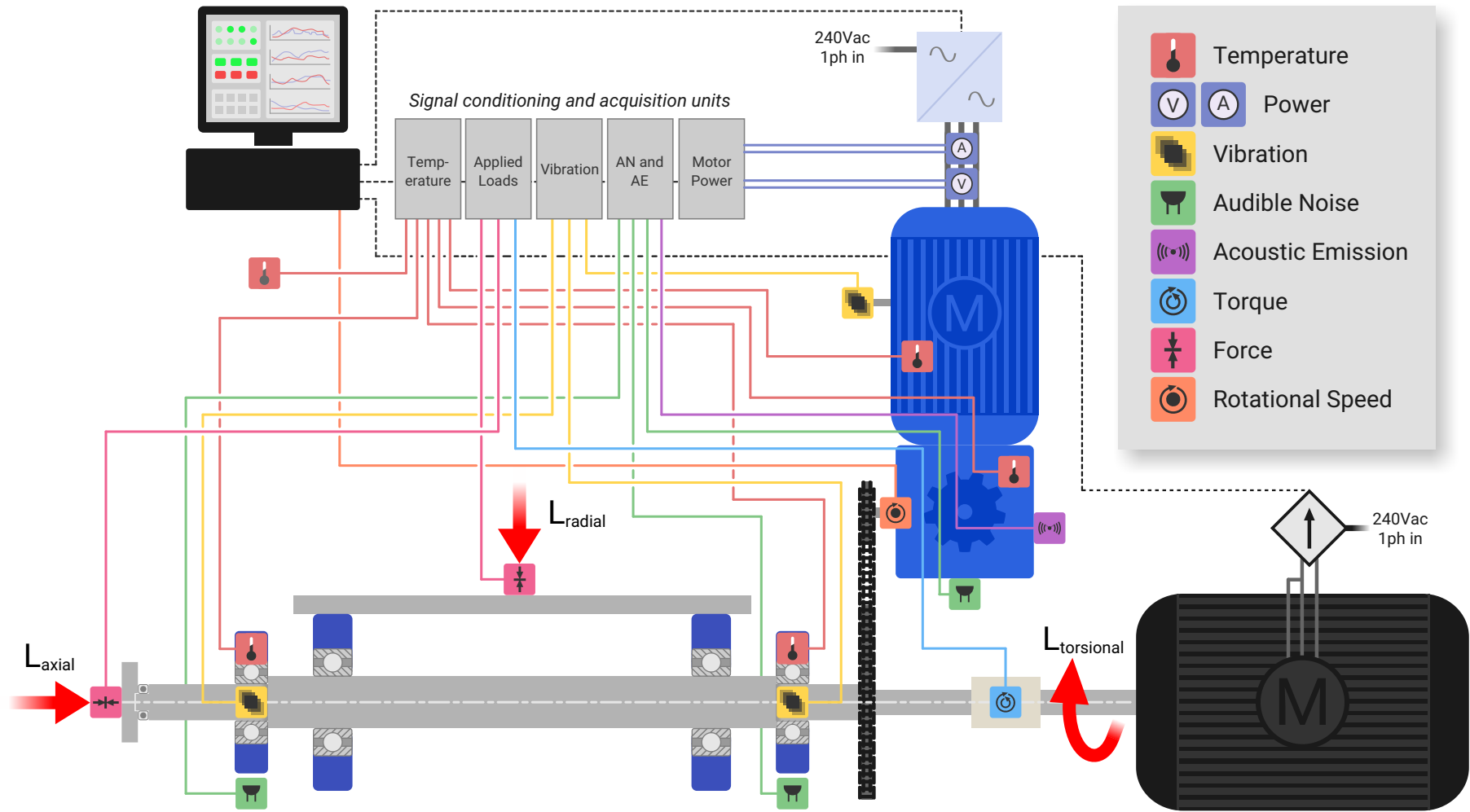
Figure 5: CER instrumentation schematic

The figure shows a CER instrumentation schematic including a computer display, signal conditioning and acquisition units (Temperature, Applied Loads, Vibration, AN and AE, Motor Power), a 240Vac 1ph in power supply, motors, bearings, and various sensors. Labels include L_{radial}, L_{axial}, $L_{torsional}$, and 240Vac 1ph in.

Legend:
- Temperature
- Power (V and A)
- Vibration
- Audible Noise
- Acoustic Emission
- Torque
- Force
- Rotational Speed

3. Testing Regime

3.1. Operational Procedure

Test scenarios are commenced from a cold start, with all primary rig parameters allowed to reach a steady state condition each time an operational condition (speed/load) changes. Consistent steps in speed and load are used during test scenarios (table 7) to support repeatability. A 3kN maximum limit on applied radial loading is specified to prevent significant deflection of the drive shaft, minimising the potential for plastic deformation or even complete fracture.

Table 7: Summary of magnitudes of testing variables used

Variable	Abbrev.	Step 1	Step 2	Step 3
Speed (Hz)	S	15	30	45
Axial Load (kN)	A	2	4	6
Radial Load (kN)	R	1	2	3
Torsional Load (Adc)	T	2	5	8

Durations of test scenarios are dictated by the time required for parameters to reach steady state conditions in response to operational changes, and each scenario is run 3 times to confirm repeatability of observations.

To minimise the impact upon system dynamics of component wear or replacements between test scenarios the rig is run through a baselining test. If any significant changes in system parameters during unloaded operation are observed, then the relevant component(s) are replaced by fresh components to maximise consistency between scenarios.

3.2. Characterisation of Operational Envelope

The purpose of this phase of testing aims to profile the response of system parameters to changing speed and load conditions. As presented in table 8 these conditions are applied over 8 scenarios, encompassing variation in speed, radial, axial, and torsional load.

3.3. Seeding of Fault Conditions

The second phase of testing is designed to enable the seeding of the failure and fault conditions described in section 2.1, for the purpose of assessing the degree to which each monitored system parameter is able to detect the presence of each seeded condition. Data collected from the test rig aims to be as reflective of typical conveyor operation as possible, therefore the scenarios implemented are based upon observations of issues observed in industrial operations, as opposed to the trivial nature of faults typically seeded within literature.

Table 8: Summary of operational characterisation test scenarios

ID	Description	Mode of Loading	Loading Profile	Rationale	Method
PTR_TS_A	Multi speed characterisation	None	NA	Characterise unloaded operation.	Run at 15 30 45Hz sequentially.
PTR_TS_B	Radial loading of drive shaft	Radial	Step	Emulate increased belt tension.	Run at 45Hz, apply 1 2 3kN sequentially.
PTR_TS_C	Axial loading of drive shaft	Axial	Step	Emulate uneven belt tracking.	Run at 45Hz, apply 1 2 3kN sequentially.
PTR_TS_D	Combined radial and axial loading	Radial Axial	Constant Step	Emulate increasing belt tension with uneven belt tracking.	Run at 45Hz, apply 3kN radial, then apply 2 4 6kN axial sequentially.
PTR_TS_E	Torsional loading of drive shaft	Torsional	Step	Emulate increasing levels of product on belt.	Run at 30Hz, apply 3 5 8A power to braking motor sequentially.
PTR_TS_F	Torsional loading of drive shaft	Torsional	Cyclic	Emulate typical profile of product being loaded.	Run at 30Hz, apply triangle wave current profile at 3 5 8A peak.
PTR_TS_G	Combined radial and torsional loading of drive shaft	Radial Torsional	Constant Step	Emulate increased belt tension during fluctuating product level.	Run at 30Hz, apply 3kN radial, then apply triangle wave current profile at 3 5 8A peak.

To maximise legitimacy of data 'natural' faults would be generated on the rig (i.e. damage generated cumulatively as a result of applied loading, rather than seeding damage) however, due to the timescales associated with inducing such damage, at this stage in the research focus shall be confined to seeded conditions. For example, a shielded, grease lubricated SKF YAR 204-2F bearing is estimated to have an operational life of 3250hrs when subject to 3kN of constant axial and radial load, rotating at 180RPM. As described in table 9 the scenarios seeded on the rig are a combination of artificial damage and manipulation of the operational environment.

Table 9: Summary of seeded fault test scenarios

Scenario ID	Description	Mode of loading	Loading profile	Rationale	Method
PTR_TS_H	Corroded bearing	Radial	Step	Emulate bearing exposed to wet environment.	Bathe bearing in saline solution for 72hrs. Install at location B and run at 15 30 45Hz. Apply 3kN radial load when at 45Hz.
PTR_TS_I	Poorly maintained bearing	Radial	Step	Emulate poorly maintained bearing being operated.	Bathe bearing in Acetone for 72hrs. Install at location B and run at 15 30 45Hz. Apply 3kN radial load when at 45Hz.
PTR_TS_J	Damaged bearing seal	Radial	Step	Emulate damage to bearing seal.	Seed defect in seal at inner race using metal punch. Install at location B and run at 15 30 45Hz. Apply 3kN radial load when at 45Hz.
PTR_TS_K	Overloaded bearing	Radial	Step	Emulate bearing damaged during installation.	Statically load bearing inner race with 25kN using Instron machine. Install at location B and run at 15 30 45Hz. Apply 3kN radial load when at 45Hz.
PTR_TS_L	Contaminated bearing	Radial	Step	Emulate metallic debris present within bearing races.	Mill hole in bearing seal and insert steel filings. Run at 15 30 45Hz. Apply 3kN radial load when at 45Hz.
PTR_TS_M	Thermal inhibition	Torsional	Step	Emulate product buildup around motor and gearbox.	Cover motor and gearbox with insulating foil. Run at 30Hz. Apply 2 5 8A constant current.
PTR_TS_N	Gearbox breather blockage	Torsional	Step	Emulate breather tube blockage.	Remove gearbox plug. Run at 30Hz. Apply 2 5 8A constant current.
PTR_TS_O	Damaged gearbox	Torsional	Step	Emulate cumulative buildup of metallic debris in gearbox from tooth wear.	Run at 30Hz. Remove plug and insert steel filings. Apply 2 5 8A constant current.

3.3.1. Bearings

Five bearing damage scenarios were seeded on the rig, a mixture of single point and distributed damage, as described by[23]. Damage was created using a variety of methods, as described in table 10.

Table 10: Summary of bearing faults artificially seeded

Fault ID	Damage type	Location	Method
BF1	Corrosion	Distributed	Bathe bearing in Acetone solution
BF2	Lubricant removal	Distributed	Bathe bearing in saline solution
BF3	Seal deformation	Single point	Deform seal using metal punch
BF4	Brinneling/Overload	Distributed	Statically load inner race against outer in axial direction (25kN)
BF5	Debris contamination	Distributed	Mill access hole in seal and insert steel filings

3.3.2. Drive System

Three fault scenarios were seeded within the test rig drive system, as described within table 11.

Table 11: Summary of drive system faults artificially seeded

Fault ID	Scenario	Method
DS1	Thermal inhibition of motor and gearbox	Encase motor and gearbox in shroud of insulating foil
DS2	Blocked breather	Remove gearbox breather plug, run rig at 45Hz until SS reached. Insert breather plug
DS3	Debris contamination	Run rig at 45Hz until SS reached. Remove breather plug and insert steel filings. Replace breather plug

4. Results

A total of total of 48 scenarios were run on the test rig, representing more than 250hrs of operation, with each scenario generating over 100 directly measured or derived parameters. As such, for brevity, exhaustive results are omitted from this paper, with only salient data presented and discussed.

4.1. *Operational Characterisation*

In response to changes in operational speed the majority of parameters present sensitivity (fig. 6). The power drawn by the drive motor increases almost linearly with increasing speed demands. Similarly, the step changes in speed can be clearly identified in the root-mean-square (RMS) value of the vibration, audible noise (AN) and acoustics emission (AE) waveforms, with the exception of the motor vibration RMS, which peaks at S2 before reducing at S3 to a value similar to S1. This is likely explained by the mounting configuration of the sensor, with the adapter used to mechanically couple the sensor to the motor casing likely producing a filtering effect on the vibration recorded at S3.
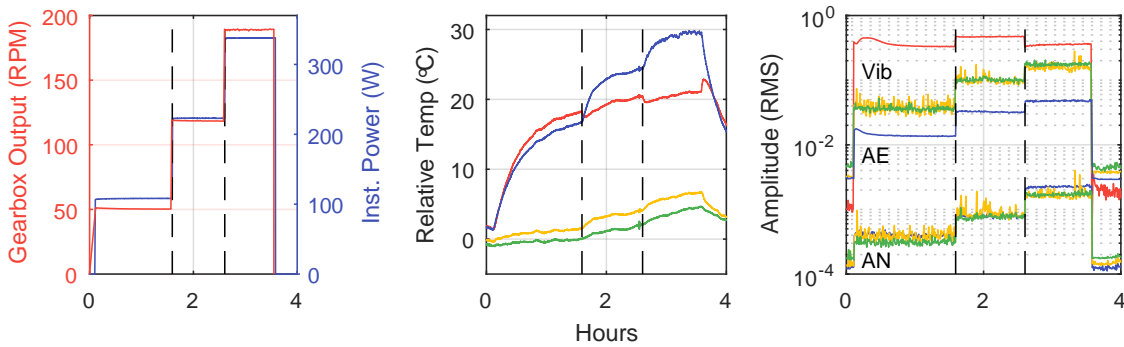

Figure 6: Multispeed characterisation test scenario. Changes in demanded speed indicated by vertical dashed lines

The temperature of all monitored components also rises in response to increases in operational speed, however in a less linear manner, with a reduction in the magnitude of the temperature increase seen from S2-S3 compared to S1-S2. Additionally, and as expected, temperature responses present significant delay in reaching a steady state, with each presenting an approximately first order response with a time constant of 49mins. The response of the motor temperature can also be observed to present stable, non-minimum phase characteristics i.e. initially, the direction of the temperature response opposes that of the change in speed[24].

In the case of the motor temperature response such behaviour can be explained by the construction characteristics of the motor. To increase the rotor speed the motor must consume more power, which, due to thermal inefficiency (i.e. Joule heating) results in a corresponding increase in heat generation within the motor core. However, as the motor temperature is monitored using a case mounted sensor this increased heat is not immediately observed, but instead time-delayed. To actively cool the motor a fan is directly mounted to the rotor to provide forced convection. As the fan is rigidly coupled to the rotor, it provides an immediate increase in airflow and thus convective power in response to an increase in

rotor speed, which is observed with minimal delay by the externally mounted temperature sensor. Thus, the response of the motor casing temperature to speed variation is the summation of a fast response, non-minimum phase component (i.e. fan action), which acts to remove heat, and a slow response, minimum phase component (i.e. heating losses) that acts to add heat.

When the test rig is subjected to an axial load in isolation a decrease in drive speed of around 1rpm per 2kN of load can be observed, however there is no corresponding increase in power consumption. Due to the open-loop operation of the VFD it makes no attempt to compensate for the reduction in speed caused by the application of axial load. Accordingly, little change in the RMS value of the motor and gearbox vibration, audible noise and acoustic emission is seen, and only a small increase of 1°C in the temperature of each at 6kN axial load.
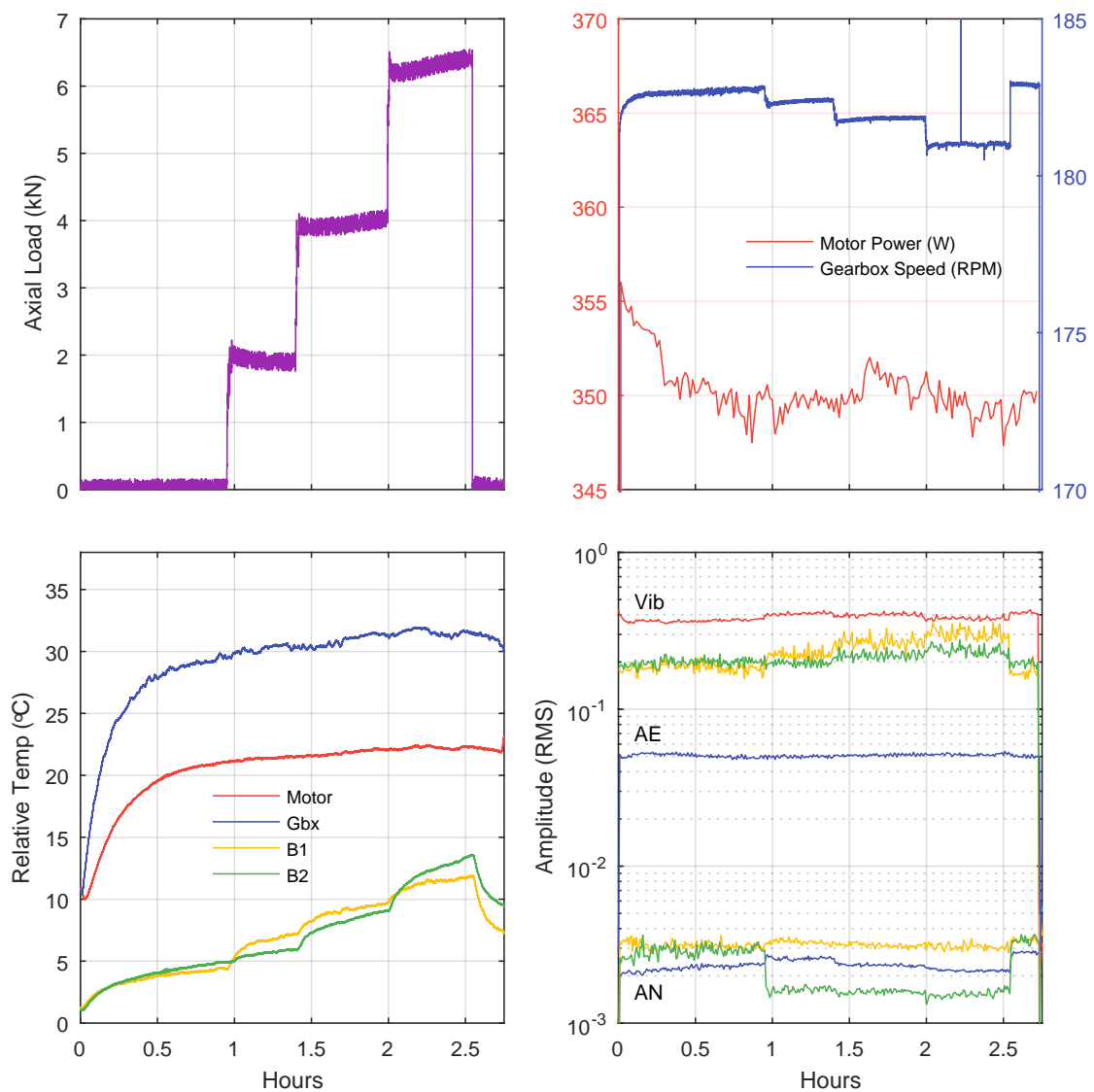
Figure 7: Axial loading characterisation test scenario

In contrast, the temperature of the main bearings present a significant increase in response to axial load. Initially, the temperature of bearing 1 increases at a greater rate than bearing 2, rising by 2.5°C from 0-2kN, compared to 1°C for bearing 2. Due to the stepped profile present on the drive shaft and the direction in which axial load is applied, much of the load is reacted by bearing 1, thus it experiences increased frictional losses resulting in the temperature rise observed. In contrast, bearing 2 is axially constrained to the drive shaft by just two grub screws, hence it reacts only a fraction of the applied load and so experiences less increase in heat.

However, as the applied load is increased from 2-4-6kN, whilst bearing 1 presents a further 2 steps of 2.5°C, bearing 2 presents steps of 2.5°C and 5°C respectively. This behaviour can be explained by the design of the test rig. Axial load is transferred to the drive shaft via a needle roller thrust bearing to minimise parasitic torsional force. However, as a consequence the motion of the thrust bearing generates heat via frictional losses, proportional to the applied load, which is added into the system. Thermal images taken during tests indicate that a temperature of around 70°C was reached at the thrust bearing's location, which eventually causes an artificial increase in the temperature of bearing 2 as heat is conducted through the shaft.
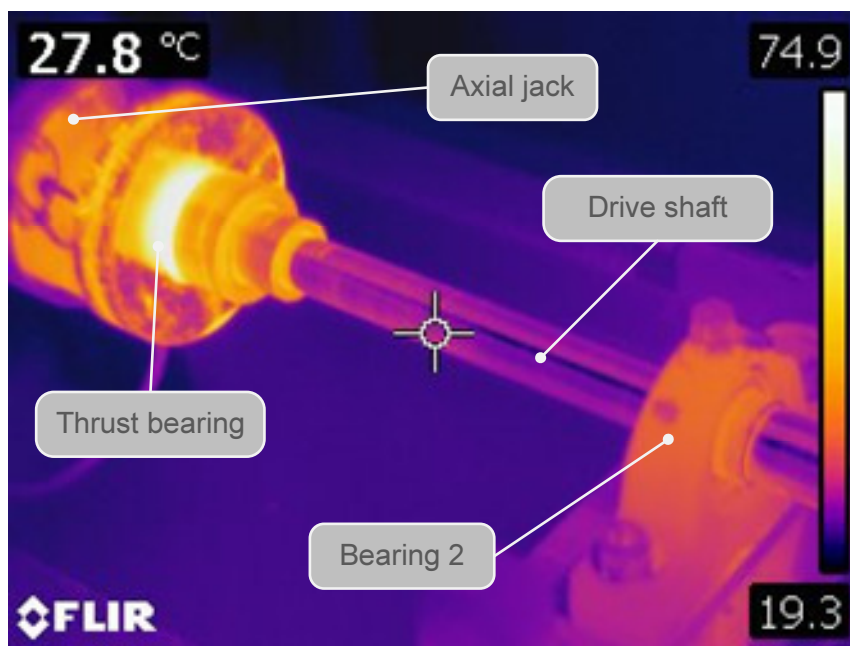

Figure 8: Thermal image of drive shaft and axial loading location during the application of 6kN axial load - note maximum scale temperature of 74.9°C

The vibration RMS value of each bearing shows an increase at each step of axial load applied, with bearing 1 values slightly greater, as a result of supporting more load. The audible noise RMS value of bearing 1 shows little sensitivity to applied axial load, however bearing 2 presents a clear drop across the range of axial load.
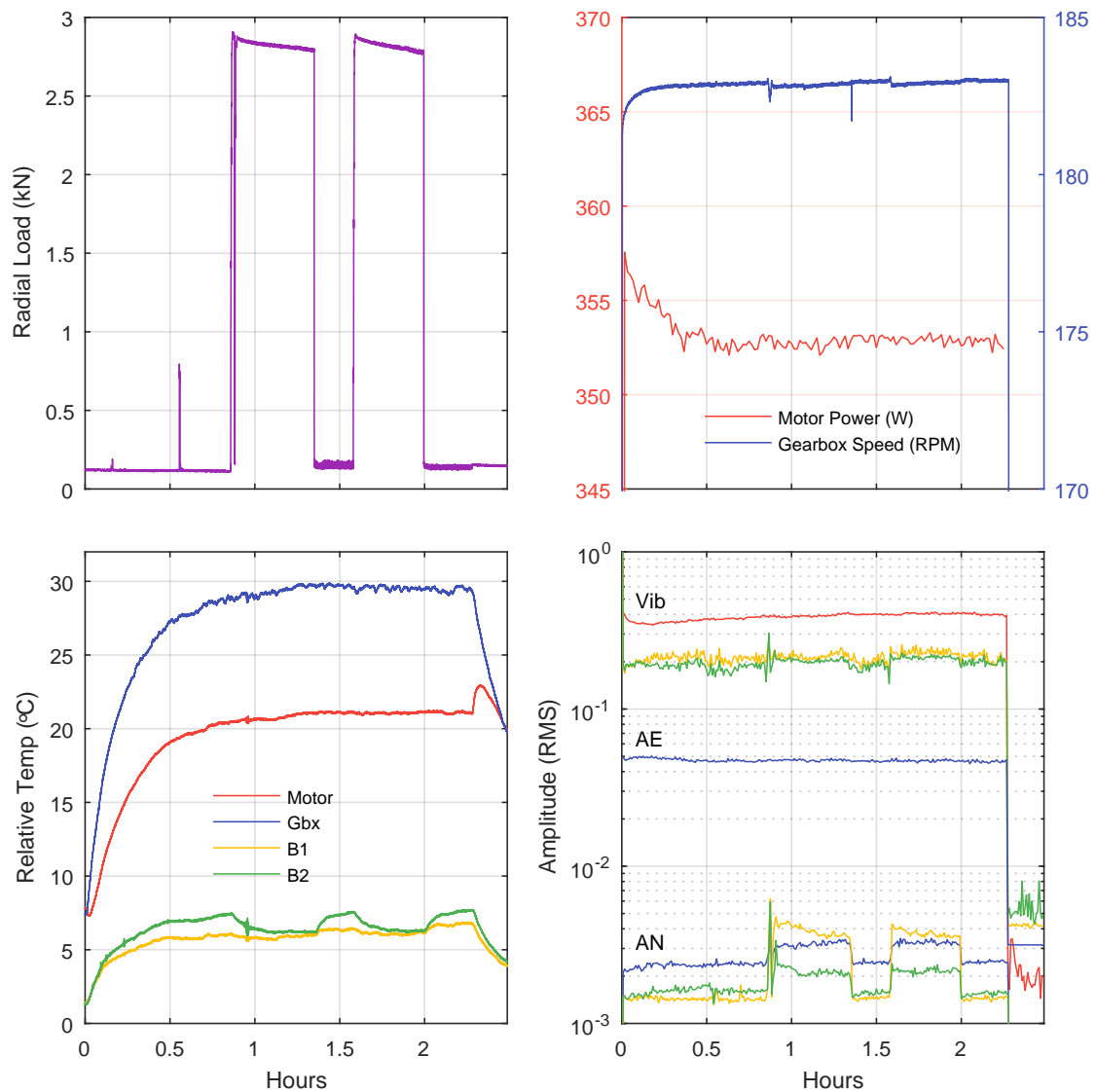
Figure 9: Radial loading characterisation test scenario

As with the application of axial load, radial load applied in isolation is not supported mechanically by the test rig drivetrain and thus induces little change in motor and gearbox parameters, with no significant change in speed, power consumption, temperature, RMS vibration or RMS acoustic emission observed across the applied range.

Both main bearings show a small reduction in temperature and vibration RMS value as radial load is applied, with the applied load producing a constraining effect, however a significant increase in audible noise of both bearings and the gearbox can be seen in the presence of radial load. This increased noise is generated by the chain drive; in response to the application of radial load the drive shaft deflects causing a reduction in the centre distance of the sprockets. This, in turn, causes a slackening of the chain and thus an increase in noise.
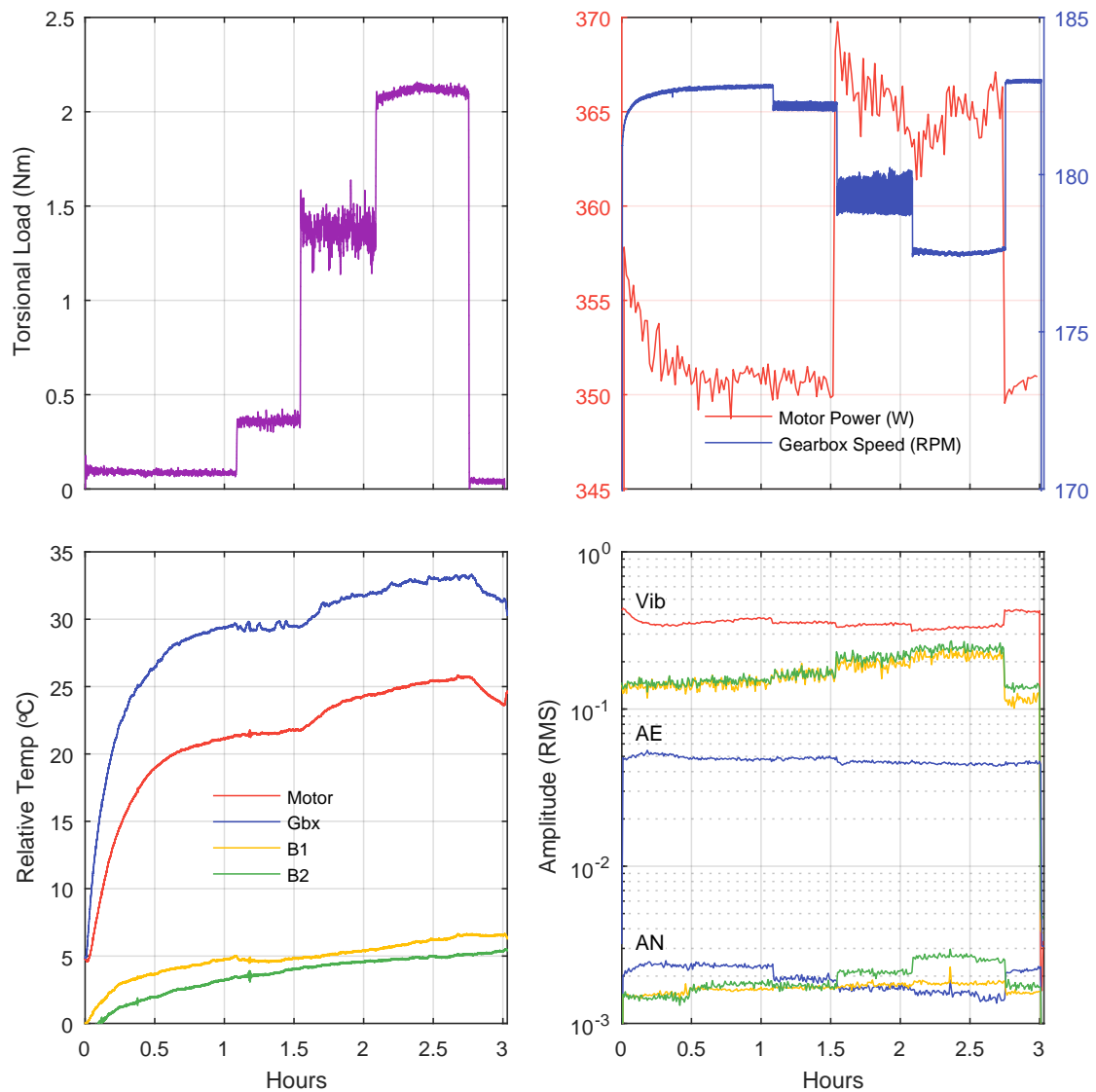
Figure 10: Torsional loading characterisation test scenario

In contrast to the application of axial and radial load, torsional load is reacted by the motor and gearbox. As such, the application of torsional load causes a simultaneous decrease in speed and increase in power consumption of 5rpm and 15W respectively. An increase of 5°C can also be observed in the response of both the motor and gearbox to 2Nm of torsional load, however, this corresponds with a reduction in the motor vibration and gearbox audible noise RMS values, as a result in the reduction in speed.

Neither of the main bearings present significant temperature sensitivity to torsional load, however vibration and audible noise RMS levels do increase as torsional load is stepped up. This is likely a result of the increased noise generated by the chain under torsional load, reflected in the greater magnitude of bearing 1 audible noise compared to bearing 2.
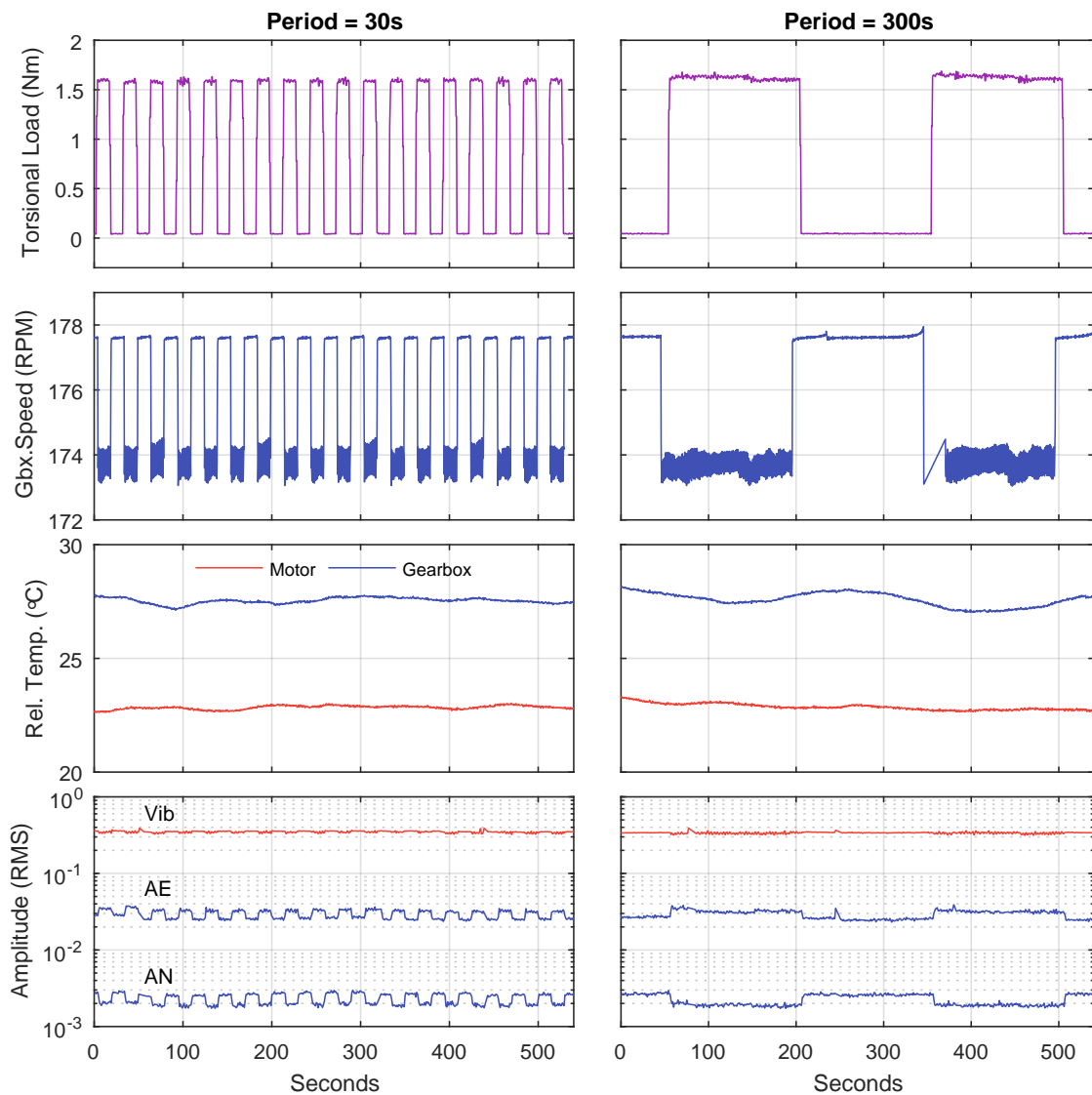
Figure 11: Torsional square-wave loading characterisation test scenario

When subject to a triangle-wave torsional load profile, the filtering effect of thermal inertia can be observed in the response of the motor and gearbox temperatures. Whilst the response of the speed, load, vibration, AN and AE RMS parameters present little phase delay in response to changes in torsional load, the temperature of the motor and gearbox presents both lag and smoothing. This effect becomes more apparent as the period of the input profile is increased (fig. 11).

4.2. Fault Scenarios

Across all bearing fault scenarios no significant sensitivity in any motor or gearbox parameters can be observed (fig. 12).
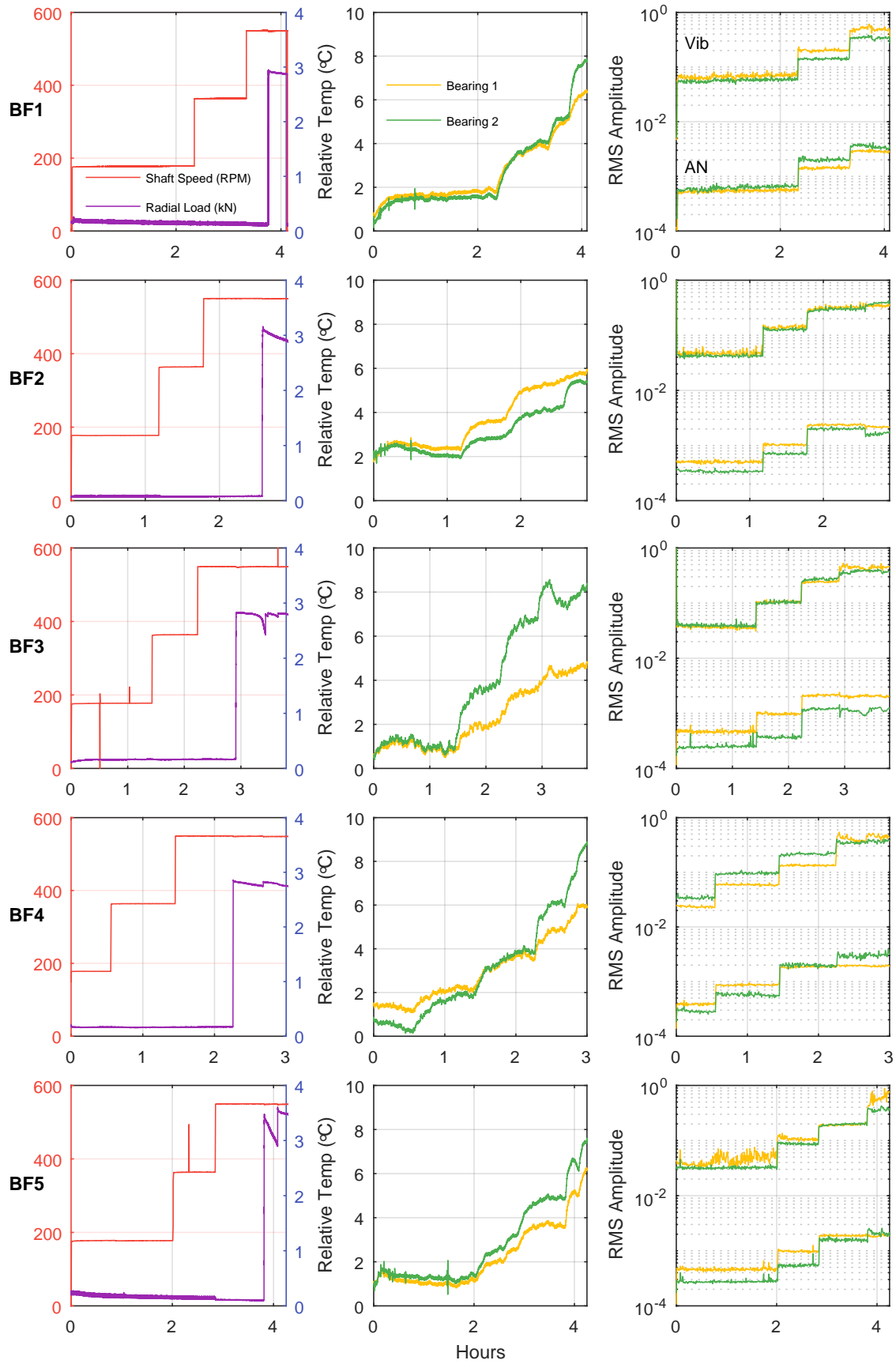
Figure 12: Bearing fault test scenarios

However, all faulty bearings present an increased temperature compared to the healthy bearing 1 baseline shown in fig. 6. Additionally, all bearing differential temperatures show the faulty bearing (bearing 2) under test exceeding the associated healthy bearing (bearing 1), with the exception of BF2. This is likely explained by the nature of the fault; the removal of lubricant likely enables more heat to be radiated away from the contact surfaces. However, the differential of BF2 can be seen to reverse as radial load, demonstrating the purpose of lubricant in reducing frictional losses and thus heat generation.

Differential vibration RMS values across bearing faults are mostly negligible. BF4 does show an increased level of vibration however this doesn't persist when radial load is applied. Similarly, most audible noise RMS differentials are not significant or consistent, with any differentials present prior to load often reversing once radial load is applied. Typically, bearing 1 presents a greater audible noise RMS value than bearing 2, likely as a result of its proximity to the drive chain.

In response to artificial thermal inhibition of the drivetrain only the motor and gearbox temperatures show significant sensitivity, with each increasing by 27°C and 16°C respectively, after a sharp initial rate of change.
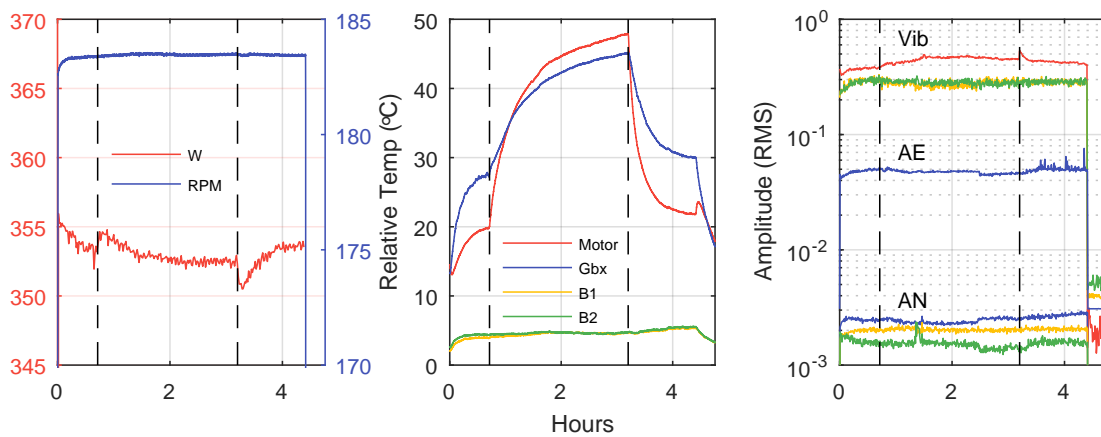

Figure 13: Thermal inhibition of the drive system test scenarios

No significant change in speed or power consumption of the motor is seen, despite the restricted airflow. A small increase in motor vibration RMS and decrease in gearbox AN RMS does also result, as an effect of the presence of the insulating cover.

Operating the rig with the gearbox breather plug removed causes little effect on any monitored parameters, despite a quantity of gearbox oil being observed to escape whilst the plug was removed (fig. 14).
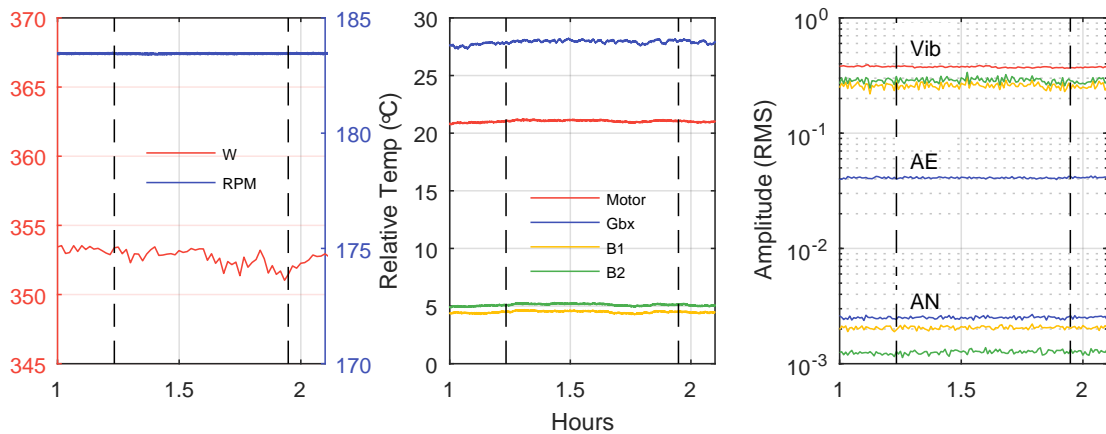
Figure 14: Insertion and removal of gearbox breather plug test scenarios

In response to the insertion of metallic debris in the gearbox a small increase (1°C) in the temperature of both the motor and gearbox is seen. However, a far more significant increase in the RMS value of both the motor vibration and gearbox AE can also be seen. No significant sensitivity is seen in any bearing parameters.
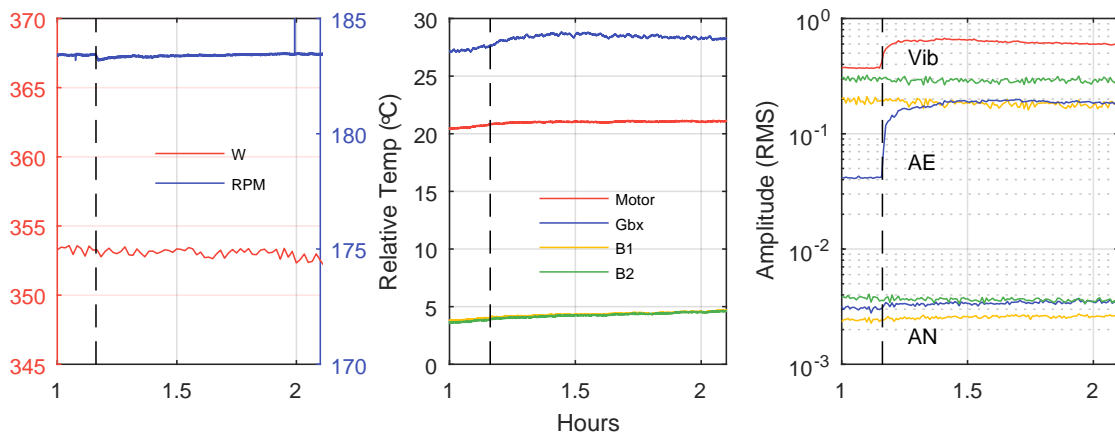

Figure 15: Insertion of debris into gearbox test scenarios

5. Discussion

When applied in isolation, from the data acquired during tests identification of both the presence of and form of the loading applied is indicated in the response of specific combinations of parameters (table 12).

Such understanding could support operators in assessing the usage of a system in real-time, enabling more informed PPM intervals to be scheduled, based upon how the operation of the system is changing rather than purely operational hours. Initially, this could be implemented through encoding understanding within thresholds of system parameters to simplify interpretation by operators, however a more detailed and evidenced understanding of behaviours is likely to be required in order to mitigate the issues associated with determining appropriate thresholds across multiple assets[25],[26],[27].

Table 12: Summary of sensitivity of parameters to applied loading profiles

Applied Loading	Sensitive parameters	Response
Axial	B1 temp, B2 temp, B1 vib, B2 vib, B2 AN,	Bearing temperature and vibration RMS differential present - B1 greater than B2. Reduced B2AN RMS under load
Radial	B1 temp, B2 temp, B1 AN, B2 AN	Decrease in absolute temp and increase in AN RMS of both B1 and B2
Torsional	Motor temp, gbx temp, motor vib RMS, gbx AN and AE RMS, motor power, gbx speed	Increased power drawn with decreased gbx speed. Increases in all other parameters

The degree of confidence associated with identification of loading conditions can be considered a function of the quantity and quality of operational information available. For example, one can be more confident in stating that an axial load is present by using both temperature and audible noise data as opposed to temperature data alone. Whilst this may increase confidence in the inference made it also increases the data acquisition requirement associated with a system, bringing both added cost and complexity to the system[11],[7]. Therefore, the value of such inferences to operators should be assessed, likely dependent upon how much correlation between the operational usage and failure of a system can be observed.

In addition, loading conditions have been considered only in isolation, that is, it is assumed only a single loading condition is ever present. In actuality there is nothing preventing a conveyor system being subjected to multiple modes of loading simultaneously, which is likely to influence negatively upon the accuracy of the inference able to be made.

Therefore, quantifying system usage in terms of the cumulative work done by the system may provide a more accurate metric for maintenance interval scheduling over purely cumulative operational hours. The total work done by a conveyor in moving product is a function of the power required to move the product and the distance the product is moved i.e.

$$\int_{t_0}^{t_n} P_{in} \cdot v_{belt} \, dt$$

Where P_{in} is the instantaneous power consumed by the drive motor and ν_{belt} is the speed of the belt.

Typically, PPM actions are applied to assets which have been observed to present age-related failures, with intervals defined based upon heuristic understanding of the mean time between failures (MTBF). Intervals defined in such a manner neglect the impact of intensity of usage on failure, therefore by utilising both the intensity of work as well as the quantity more accurate intervals may be identifiable. However, whilst observing the intensity of operation does neglect the effect this may have on the health of a system. For
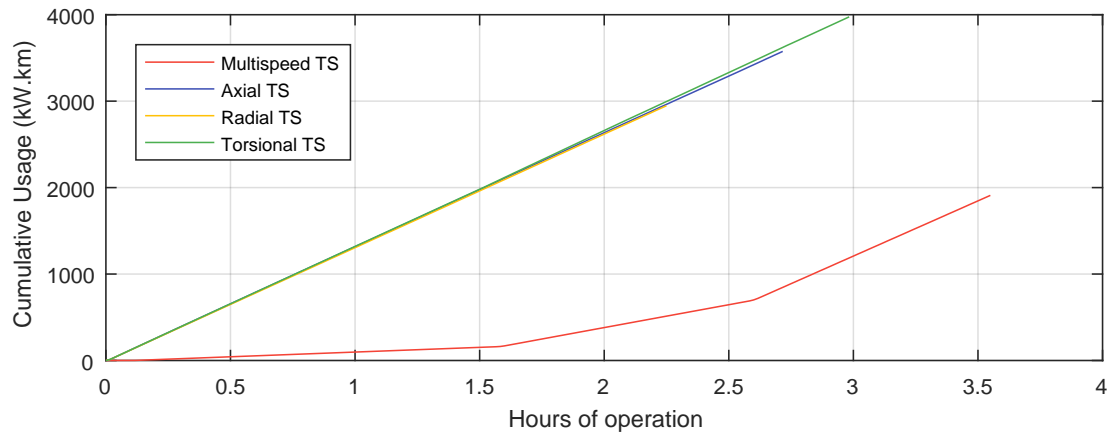
Figure 16: Cumulative usage during isolated loading test scenarios

example, does operating at 100% load for 1 hour have the same impact upon asset health as operating at 100% load for 10 hours? Understanding such relationships is key to realising maximum asset life whilst minimising unplanned downtime, a task which will require a comprehensive dataset, compiled from the in situ operation of typical industrial conveyor systems. Similarly to the identification of operational state, the level of inference able to be made about the occurrence of fault conditions is dependent upon the range of information available. Data acquired during the seeding of faults enables indicators of the presence of faults seeded to be identified, as summarised in table 13.

Fault detection may be possible from a single parameter alone e.g. an increase in motor temperature can indicate a fault is present within the system, however, there is a significant degree of ambiguity in such a single source inference.

As indicated in fig. 17 the increase observed could be a response to a number of scenarios, such as a change in rotor speed, increased torsional load or thermal inhibition, and without more extensive information it is not possible to accurately determine whether a change in operation or a fault has occurred, and if so, type it. Additionally, as with applied loading conditions, faults have been seeded in isolation. The addition of having potentially multiple loads and faults present simultaneously within a system further increases the complexity of fault detection, isolation and typing tasks.

Table 13: Summary of sensitivity of parameters to the presence of seeded fault conditions

Fault Scenario	Sensitive parameters	Response
Gearbox with debris injected	Motor vib RMS, gbx AE RMS and temp	Increase in all as debris introduced
Gearbox breather blocked	-	-
Drive thermally inhibited	Motor, gbx temp	Increase in both without speed or power change
Corroded bearing	B2 temp, B2 AN RMS	Increase in both relative to B1
Delubricated bearing	B2 temp	Decrease in B2 compared to B1
Bearing seal damage	B2 temp, B2 AN RMS	Increase in temp decrease in AN of B2 compared to B1
Axially overloaded bearing	B2 temp, B2 AN RMS	Increase in temp and AN of B2 compared to B1
Bearing with debris injected	B2 temp, B2 AN RMS	Increase in temp and AN of B2 compared to B1

Additional data may support inferences at these lower levels, observed either directly or identified via advanced signal processing techniques. For example, AN RMS values of BF4 and BF5 were similar during tests and thus it could be inferred that typing between the two is not possible. However, during testing an audible differential between the two scenarios could be identified to the ear, therefore by using frequency domain-based signal processing techniques such typing may be possible. Again, increasing the volume of data available describing such scenarios within industrial settings will be vital in increasing accuracy and confidence in such inferences, supporting the development of probabilistic models of failure.

6. Conclusions

The data acquired during tests completed on the Conveyor Emulation Rig (CER) as presented has suggested that both changes in operational state as well as the occurrence of specific fault scenarios can feasibly be identified from certain system parameters. Data suggests that each parameter monitored presents sensitivity to specific scenarios, however no single parameter can provide valuable insight in all scenarios. Additionally, the level of insight possible varies across parameters, with accurate insight at the isolation and typing levels typically requiring the leveraging of information from multiple parameters in conjunction with historical failure observations.

At this stage, data suggests that detection of the faults explored may be possible using a
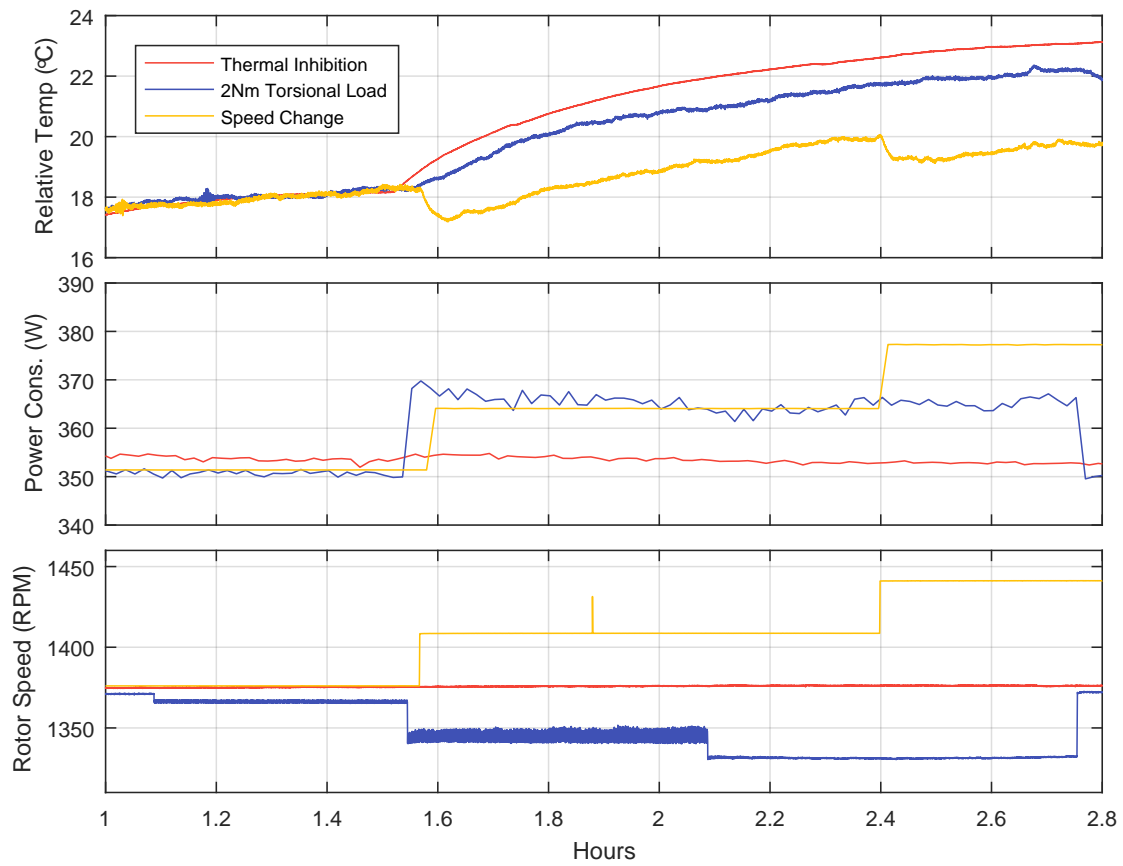
Figure 17: Comparison of motor temperature response to various changes in operation

combination of speed, power and temperature parameters alone. However, there is a non-trivial cost associated with obtaining the information required to make these inferences, potentially which far exceeds the cost of the monitored components themselves, therefore more investigation is required to enable assessment of the value of different levels of inference to operators. Increasing the extent of sensing infrastructure incurs not only financial cost, but also increases system complexity which can require significant effort to maintain, therefore an increased understanding of the insight that can be realised by each sensor, not only in isolation but also in combination, is required before justification can be demonstrated to operators.

In this vein, further testing within both a laboratory and industrial environment is essential, not only to enable validation of the CER, but to enable an improved understanding of failures and fault scenarios. The complex dynamics of conveyor operation have thus far been isolated where possible to ease analysis, however to maximise validity of data, and thus value of outputs increased complexity of loading and faults must be addressed.

Acknowledgements

References

1. T. Schools. "Condition Monitoring of Critical Mining Conveyors". In: *Engineering and Mining Journal* 216.3 (2015), p. 50.

2. R. T. Swinderman et al. *Foundations - The practical resource for cleaner, safer, more productive dust & material control*. Martin Engineering, 2009, p. 574.

3. A. J. J. Braaksma, W Klingenberg, and J Veldman. "Failure mode and effect analysis in asset maintenance: a multiple case study in the process industry." In: *International Journal of Production Research* 51.4 (2013), pp. 1055–1071.

4. D Fonseca. "An expert system for reliability centered maintenance in the chemical industry". In: *Expert Systems with Applications* 19.1 (2000), pp. 45–57.

5. J. Igba et al. "A Systems Approach Towards Reliability-Centred Maintenance (RCM) of Wind Turbines". In: *Conference on Systems Engineering Research*. Vol. 16. Elsevier B.V., Jan. 2013, pp. 814–823.

6. D. Kwon et al. "IoT-Based Prognostics and Systems Health Management for Industrial Applications". In: *IEEE Access* 4 (2016), pp. 3659–3670.

7. W. W. Tiddens, A. J. J. Braaksma, and T. Tinga. "The Adoption of Prognostic Technologies in Maintenance Decision Making: A Multiple Case Study". In: *Procedia CIRP* 38 (2015), pp. 171–176.

8. J. Moubray. *Reliability-centered Maintenance 2.1 (2nd Edition)*. 2nd. Oxford: Butterworth-Heinemann, 1997.

9. A. Starr et al. "Maintenance Today and Future Trends". In: *E-maintenance*. London: Springer London, 2010. Chap. 2, pp. 5–37.

10. R. Blazej, L. Jurdziak, and W. Kawalec. "Operational Safety of Steel-Cord Conveyor Belts Under Non-stationary Loadings". In: *Advances in Condition Monitoring of Machinery in Non-Stationary Operations. Applied Condition Monitoring*. Ed. by F. Chaari et al. Vol. 4. Springer International Publishing, 2016, pp. 535–544.

11. O. Freeman Gebler et al. "Towards the implementation of a predictive maintenance strategy : Lessons learned from a case study within a waste processing plant". In: *European Conference of the Prognostics and Health Management Society 2016*. 2016, pp. 1–17.

12. G. Lodewijks et al. "An Application of the IoT in Belt Conveyor Systems". In: *Internet and Distributed Computing Systems. IDCS 2016*. Ed. by Wenfeng Li et al. Vol. 9258. Springer, Cham, 2016, pp. 340–351.

13. A. Heng et al. "Rotating machinery prognostics: State of the art, challenges and opportunities". In: *Mechanical Systems and Signal Processing* 23.3 (Apr. 2009), pp. 724–739.

14. A. K. S. Jardine, D. Lin, and D. Banjevic. "A review on machinery diagnostics and prognostics implementing condition-based maintenance". In: *Mechanical Systems and Signal Processing* 20.7 (Oct. 2006), pp. 1483–1510.

15. I. K. Jennions. *Integrated Vehicle Health Management: Perspectives on an Emerging Field*. SAE International, 2011.

16. B. S. Iso. "Condition monitoring and diagnostics of machines — Prognostics — Part 1 : General guidelines". In: 3 (2004).

17. ISO and IEC. *ISO/IEC Directives, Part 2: Rules for the structure and drafting of International Standards*. Tech. rep. ISO, 2011, p. 76.

18. P. Tavner et al. *Condition Monitoring of Rotating Electrical Machines*. 2nd. The Institute of Engineering and Technology, 2008, p. 304.

19. B. Lu, T. G. Habetler, and R. G. Harley. "A nonintrusive and in-service motor-efficiency estimation method using air-gap torque with considerations of condition monitoring". In: *IEEE Transactions on Industry Applications* 44.6 (2008), pp. 1666–1674.

20. R. L. Rusby. *Introduction to Temperature Measurement*. Tech. rep. 125. National Physical Laboratory, 2015.

21. P. Theobald, B. Zeqiri, and J. Avison. "Couplants and their Influence on AE Sensor Sensitivity". In: *Journal of Acostic Emission* 26 (2008), pp. 91–97.

22. ISO. *ISO 13373-1:2002 - Condition monitoring and diagnostics of machines — Vibration condition monitoring — Part 1 : General procedures*. 2002.

23. C. Lessmeier et al. "Condition Monitoring of Bearing Damage in Electromechanical Drive Systems by Using Motor Current Signals of Electric Motors : A Benchmark Data Set for Data-Driven Classification Condition Monitoring of Bearing Damage in Electromechanical Drive Systems". In: *European Conference of the Prognostics and Health Management Society 2016*. Ed. by I. Eballard and A. Bregon. PHM Society, 2016.

24. R. C. Dorf and R. H. Bishop. *Modern Control Systems*. Pearson Prentice Hall, 2011, p. 1082.

25. E. Bechhoefer and A. P. F. Bernhard. "A generalized process for optimal threshold setting in HUMS". In: *IEEE Aerospace Conference Proceedings* Ci (2007).

26. M. Sawicki et al. "An automatic procedure for multidimensional temperature signal analysis of a SCADA system with application to belt conveyor components". In: *Procedia Earth and Planetary Science* 15 (2015), pp. 781–790.

27. P. K. Stefaniak et al. "Diagnostic Features Modeling for Decision Boundaries Calculation for Maintenance of Gearboxes Used in Belt Conveyor System". In: *Advances in Condition Monitoring of Machinery in Non-Stationary Operations. Applied Condition Monitoring*. Ed. by F. Chaari et al. Vol. 4. Springer International Publishing, 2016, pp. 251–262.